

Derivation of the Unified Charge Control Model with Application to the Long-Channel MOSFET I-V Characteristics

Ana Isabela Araújo Cunha¹, Márcio Cherem Schneider and Carlos Galup Montoro

Departamento de Engenharia Elétrica, Universidade Federal de Santa Catarina, C.P. 476,
CEP 88040-900, Florianópolis, SC, Brazil

Phone: 55-48-2319504 Fax: 55-48-2319091

(1) Permanent address: Departamento de Engenharia Elétrica da Escola Politécnica,
Universidade Federal da Bahia, CEP 40210-630, Salvador, BA, Brazil

Abstract - The Unified Charge Control Model (UCCM) has been first presented in [1, 2] as an empirical relationship between inversion charge density and the applied voltages in the MOS transistor. This paper presents a physical derivation of the UCCM based on Boltzmann statistics, the charge sheet approximation and the linear relationship between inversion charge density and surface potential [3, 4]. Using the UCCM and the MOSFET charge model presented in [3], we develop a new MOSFET model formulated in terms of the drain current in saturation. Experimental data and the theoretical model are shown to match very well.

I. Introduction

Circuit simulation and process characterization of the present generation of integrated circuits require an analytical MOSFET model that is valid from low to high current levels. The desirable properties of this MOSFET model [5, 6] can be summarized as follows: (i) a strong physical basis, (ii) single-piece, continuous and accurate expressions, (iii) as few parameters as possible, (iv) preservation of the source-drain symmetry of the transistor.

In this work, we present a new MOSFET model that satisfies the above mentioned properties. We first derive a charge law similar to the UCCM. The latter was originally presented in [1, 2] as an empirical model. We show that the UCCM is based on Boltzmann statistics, the charge sheet approximation and the linear relationship between inversion charge density and surface potential [3, 4]. Next, we combine the new charge law and the drain current expression derived in [3] to obtain a new I-V MOSFET model. Finally, we propose a very simple procedure to extract the parameters of the new model.

II. Derivation of the Unified Charge Control Model

According to Boltzmann statistics, the inversion charge density (Q'_1) at a position x along the channel of a long-channel uniformly doped MOSFET is given by [7]:

$$Q'_1(x) = -qn_0 \int_{y_s}^{y_c} e^{[\phi(x,y) - V_c(x)]/\phi_t} dy \quad (1)$$

In (1) q is the electron charge, n_0 is the free electron concentration in equilibrium, ϕ_t is the thermal voltage, y is the coordinate perpendicular to the oxide-semiconductor interface, $\phi(x,y)$ is the electrostatic potential,

V_C is the channel potential, y_S is the value of y at the oxide-semiconductor interface and y_C is an arbitrary depth in the bulk where the electron concentration is negligible.

The charge-sheet model approach [7] allows substituting $\phi(x,y)$ by the surface potential $\phi_S(x)$, leading to the simplified form of (1):

$$dQ'_I(x) = \frac{Q'_I(x)}{\phi_t} [d\phi_S(x) - dV_C(x)] \quad (2)$$

The basic approximation of the model proposed in [3] is the incrementally linear relationship between Q'_I and ϕ_S , for constant gate-to-bulk voltage V_G :

$$dQ'_I = nC'_{ox} d\phi_S \quad (3.a)$$

In (3.a) n is the slope factor given by:

$$n = 1 + \frac{\gamma}{2\sqrt{\phi_0 + V_P}} \quad (3.b)$$

where ϕ_0 is a constant potential a few ϕ_t above or below twice the Fermi potential ($2\phi_F$). V_P is the pinch-off voltage defined as:

$$V_P = \left[\sqrt{V_G - V_{T0} + \left(\frac{\gamma}{2} + \sqrt{\phi_0} \right)^2} - \frac{\gamma}{2} \right]^2 - \phi_0$$

$$\cong \frac{V_G - V_{T0}}{n} \quad (3.c)$$

where V_{T0} is the threshold voltage in equilibrium and γ is the body effect factor.

By substituting (3.a) into (2) and integrating from an arbitrary V_C to the pinch-off voltage V_P , yields:

$$\frac{Q'_{IP} - Q'_I}{nC'_{ox}} + \phi_t \ln \left(\frac{Q'_I}{Q'_{IP}} \right) = V_P - V_C \quad (4)$$

where Q'_{IP} is the value of Q'_I at pinch-off.

The first order approximation of V_P in the right-hand side of (3.c) substituted into (4) leads to an expression which is almost identical to the UCCM [1, 2].

In Fig.1 we compare the values of the inversion charge density calculated using (4) and from the classical charge-sheet expression of $Q'_I(\phi_S)$ [7] (with ϕ_S numerically evaluated in terms of V_C). It can

be readily verified that the charge-sheet model and the charge law in (4) are almost equivalent throughout the entire inversion regime of operation.

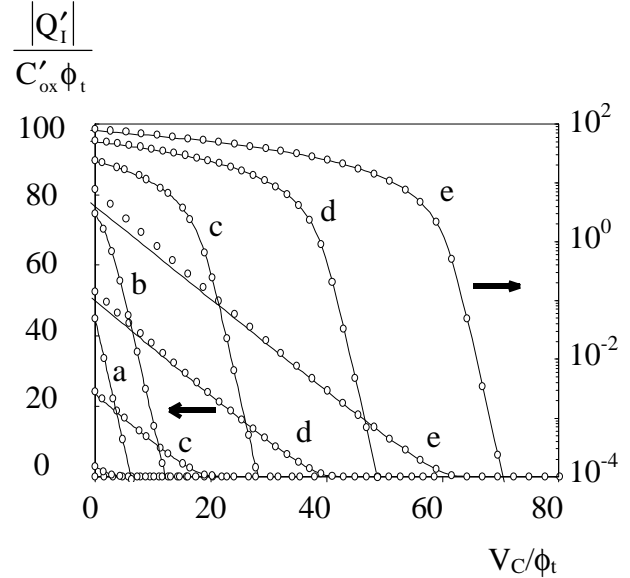


Fig.1. Normalized inversion charge density vs. normalized channel potential calculated from: (—) eqn.(4) and (o) classical charge-sheet expression with the surface potential numerically evaluated. $V_G - V_{T0}$ equal to: (a) $-5\phi_t$; (b) $5\phi_t$; (c) $30\phi_t$; (d) $60\phi_t$; (e) $90\phi_t$.

III. Long Channel I-V Modeling

In the model of [3] the expression of the drain current of a long-channel MOS transistor can be rewritten as the difference between two symmetric components:

$$I_D = I_F - I_R \quad (6.a)$$

$$I_{F(R)} = \mu C'_{ox} n \frac{W}{L} \frac{\phi_t^2}{2} \left[\left(\frac{Q'_{IS(D)}}{nC'_{ox} \phi_t} \right)^2 - 2 \frac{Q'_{IS(D)}}{nC'_{ox} \phi_t} \right] \quad (6.b)$$

where μ is the electron mobility, W is the channel width, L is the channel length and $Q'_{IS(D)}$ is the inversion charge density at source (drain). $I_{F(R)}$ is the forward (reverse) saturation current, dependent only on the gate-to-bulk voltage V_G and on the source(drain)-to-bulk voltage $V_{S(D)}$. In forward (reverse) saturation, $I_{R(F)}$ vanishes and the drain current is equal to $I_{F(R)}$.

From (6):

$$-\frac{Q'_{IS(D)}}{nC'_{ox}\phi_t} = \sqrt{1+i_{f(r)}} - 1 \quad (7.a)$$

where $i_{f(r)}$ is the forward (reverse) normalized current [6] defined as

$$i_{f(r)} = \frac{I_{F(R)}}{I_S} \quad (7.b)$$

and I_S is the normalization current, given by:

$$I_S = \mu C'_{ox} \frac{W}{L} n \frac{\phi_t^2}{2} \quad (7.c)$$

which is equal to the threshold current in saturation, I_t , defined in ref.[2, p.311], and is four times smaller than the homonym presented in [6].

Since in the model of [3] the static and dynamic characteristics are entirely formulated in terms of the inversion charge densities at source and drain and their derivatives, (7.a) enables reformulating these characteristics as functions of the forward and reverse normalized currents. The resulting model is very useful for circuit design and characterization. Furthermore, by substituting (7.a) into (4) we obtain the universal expression:

$$\frac{V_P - V_{S(D)}}{\phi_t} = \sqrt{1+i_{f(r)}} - \sqrt{1+i_P} + \ln\left(\frac{\sqrt{1+i_{f(r)}} - 1}{\sqrt{1+i_P} - 1}\right) \quad (8)$$

where i_P is the value of $i_{f(r)}$ for $V_{S(D)} = V_P$.

Expression (8) is independent of technology, transistor dimensions and temperature and demonstrates that the forward and reverse saturation characteristics (I_F vs. V_S and I_R vs. V_D) provide the same information about the MOSFET long-channel parameters.

By partially differentiating (8) with respect to the source (drain) potential, we calculate the source(drain) transconductance

$$g_{ms(d)} = -(\pm) \frac{\partial I_D}{\partial V_{S(D)}} \Bigg|_{V_G, V_{D(S)}, V_B}$$

$$g_{ms(d)} = \frac{2I_S}{\phi_t} \left(\sqrt{1+i_{f(r)}} - 1 \right) \quad (9)$$

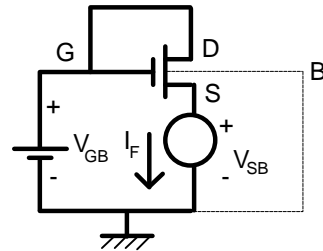
IV. Parameters Extraction and Results

The parameters of the long-channel model can be extracted using the following procedure:

a) To determine the normalization current $I_S(V_G)$, we measure the drain current in saturation ($V_D = V_G$) versus the source voltage for several values of V_G , using the circuit configuration of Fig.2.a. The ‘‘common-gate characteristics’’ thus obtained are illustrated in Figs.2.b-c for an NMOS transistor of a 0.75 μm technology, whose oxide thickness (t_{ox}) is 280 \AA and whose channel dimensions are $W = L = 25 \mu\text{m}$. From (7.b) and (9), we derive the universal relationship between the saturation current and the source-transconductance of the MOSFET:

$$\frac{I_F}{\phi_t g_{ms}} = \frac{1 + \sqrt{1+i_f}}{2} \quad (10)$$

which is independent of technology, gate voltage, transistor dimensions. The logarithmic derivative of the forward current, which corresponds to the slope of the curves in Fig.2.b is given by $\partial \ln(I_F) / \partial V_S = -g_{ms} / I_F$, thus being a function of the forward normalized current i_f , according to (10). Therefore, a particular value of the ratio I_F / g_{ms} can be used to determine I_S . The points (V_{S0} , I_{F0}) marked with an asterisk in Fig.2.b, for instance, correspond to the slope value $-2 / (3\phi_t)$ and to $i_f = I_{F0} / I_S = 3$, so that we can readily calculate $I_S = I_{F0} / 3$.



(a)

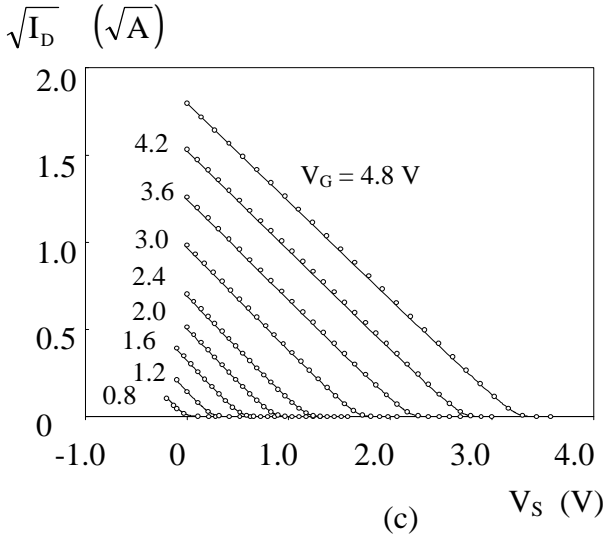
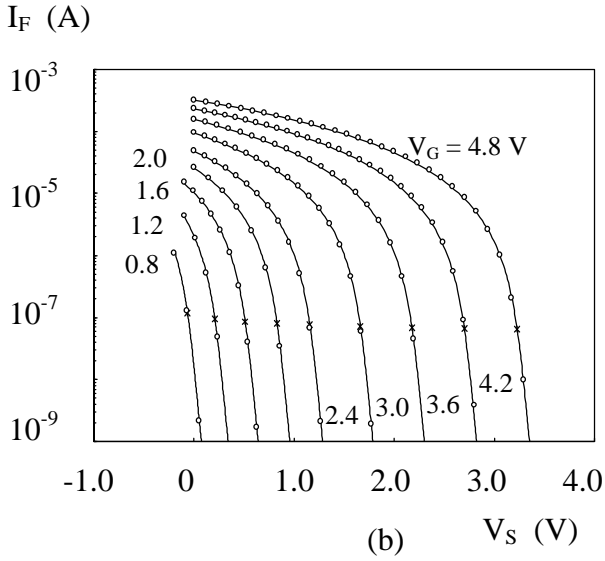


Fig.2.(a) Circuit configuration for measuring the common-gate characteristics ((b) and (c)) in saturation of an NMOS transistor with $t_{ox} = 280 \text{ \AA}$ and $W = L = 25 \mu\text{m}$: (—) simulated curves calculated from (8); (o) measured curves; (*) measured points corresponding to $g_{ms}/I_F = 2/(3\phi_t)$ and $V_S = V_P$.

The variation of the normalization current with respect to the gate voltage is illustrated in Fig.3. To a first order approximation, I_S can be assumed almost independent of V_G .

$$I_S \text{ (nA)} \quad \mu C'_{ox} \text{ (A/V}^2\text{)} \times 10^{-5}$$

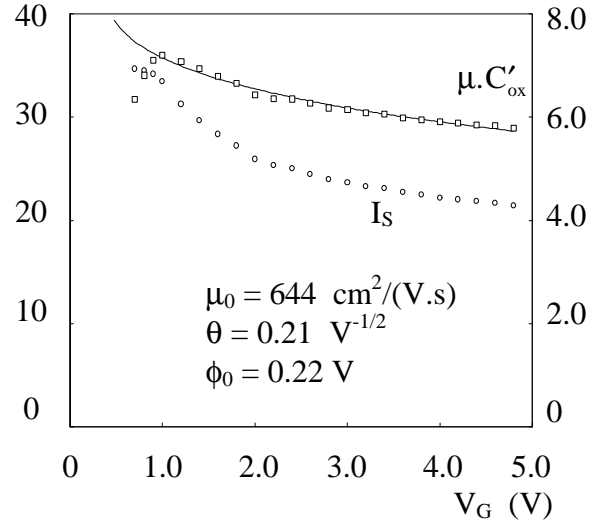


Fig.3. Normalization current and effective mobility vs. gate voltage for an NMOS transistor with $t_{ox} = 280 \text{ \AA}$ and $W = L = 25 \mu\text{m}$: (o) extracted values of I_S ; (•) values of $\mu \cdot C'_{ox}$ calculated from (10.c) using the extracted values of I_S ; (—) values of $\mu \cdot C'_{ox}$ fitted to

$$\text{the analytical expression } \mu \cdot C'_{ox} = \frac{\mu_0 C'_{ox}}{1 + \theta \sqrt{\phi_0 + V_P}}$$

b) The pinch-off voltage $V_P(V_G)$ is also extracted from the “common-gate characteristics”. According to (8), V_P is the value of V_S such that $I_F = I_{S,ip}$. Adopting, for instance, $i_p = 3$, which implies that $Q'_{IP} = -nC'_{ox}\phi_t$, V_P is equal to V_S for the points marked with an asterisk in Fig.2.b. The parameters V_{T0} , γ and ϕ_0 have been calculated by fitting the experimental curve V_P vs. V_G to (3.c), and n has been evaluated according to (3.b). Fig.4 exhibits the extracted and fitted values of the pinch-off voltage, as well as the calculated values of the slope factor.

c) The dependence of the mobility on the electrical transversal field (illustrated in Fig.3 for the same device described in (a)) can be extracted from the variations of I_S and n with respect to V_G , reporting to the definition in (7.c).

$$V_P \text{ (V)}$$

$$n$$

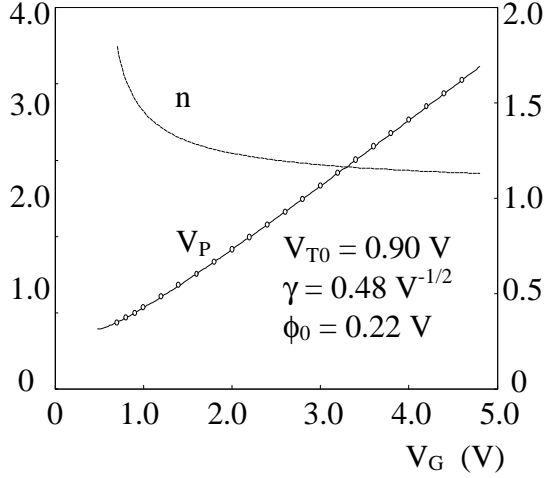


Fig.4. Pinch-off voltage and slope factor vs. gate voltage for an NMOS transistor with $t_{ox} = 280 \text{ \AA}$ and $W = L = 25 \text{ \mu m}$: (o) extracted values of V_P ; (—) values of V_P and n calculated from (3.c) and (3.b), respectively.

In Figs. 2 and 5, we compare the expressions presented in Section III with measurements. The theoretical (eqn.(8)) and measured “common-gate characteristics” in saturation are shown in Fig.2. The theoretical (eqn.(9)) and measured source-transconductances are compared in Fig.5. The experimental results fit very closely the theoretical results obtained using the model presented here.

In Fig.6, we compare the theoretical law in (10) with experimental data obtained for long-channel MOS transistors of different technologies, biased at different gate voltages. The measured points match very well the curve plotted from (10) for a wide range of i_f . Since analog circuits are generally current-biased and the current-to-transconductance ratio is an important design parameter, (10) is a very useful design tool.

g_{ms} (S)

10^{-3}

10^{-5}

10^{-7}

10^{-9}

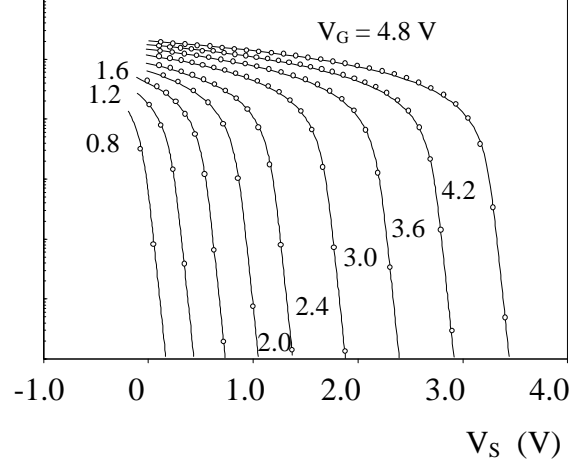


Fig.5. Source-transconductance in saturation of an NMOS transistor with $t_{ox} = 280 \text{ \AA}$ and $W = L = 25 \text{ \mu m}$: (—) simulated curves calculated from (8) and (9); (o) measured curves

I_F/g_{ms} (V)

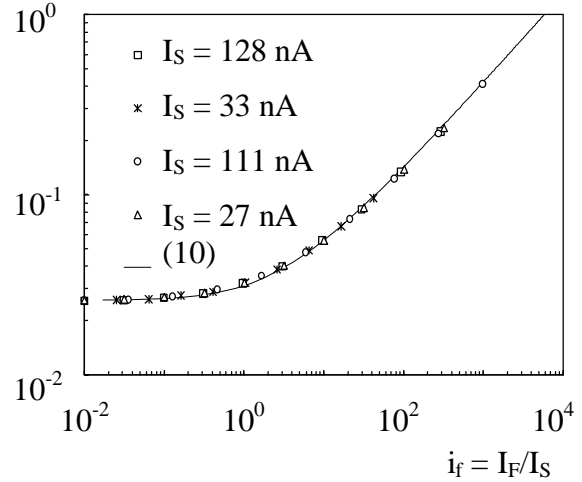


Fig.6. I_F/g_{ms} ratio vs. forward normalized current for NMOS transistors with: $t_{ox} = 55 \text{ \AA}$: \bullet ($V_G = 1.0 \text{ V}$) and \circ ($V_G = 2.0 \text{ V}$) $t_{ox} = 280 \text{ \AA}$: $*$ ($V_G = 1.0 \text{ V}$) and Δ ($V_G = 2.0 \text{ V}$) our model - expression (10): —

V. Conclusions

We have presented the physical approximation underlying the Unified Charge Control Model for MOS transistors. We have verified that the UCCM is fully consistent with

the basic approximation of the model derived in [3]. Combining the model presented in [3] with the UCCM, we have derived a MOSFET model whose key variables are the forward and reverse normalized currents. Such a feature is extremely useful, since the saturation current has a chief role in circuit performance. Moreover, the same proposed model can be simultaneously applied, without further approximations, to simulation, design and parameter extraction. The model consistence has concurred to minimize the number of parameters and to simplify their experimental determination.

Acknowledgments

The authors would like to thank the financial support of CNPq and CAPES, research agencies of the Brazilian Ministries of Science and Technology and Education. They also thank the "Laboratoire de Physique des Composants à Semiconducteur", Grenoble, for supplying the test devices.

References

[1] C-K. Park, C-Y. Lee, K. Lee, B-J. Moon, Y. H. Byun and M. Shur, "A unified current-voltage model for long-channel nMOSFET's", *IEEE. Trans. Electron Devices*, vol. 38, no.2, pp. 399-406, 1991.

[2] K. Lee, M. Shur, T. A. Fjeldly, T. Ytterdal, "Semiconductor device modeling for VLSI". Englewoods Cliffs: Prentice Hall, 1993.

[3] A. I. A. Cunha, M. C. Schneider and C. Galup-Montoro, "An explicit physical model for the long-channel MOS transistor including small-signal parameters", *Solid-State Electron.*, vol. 38, no. 11, pp. 1945-1952, 1995.

[4] M. A. Maher and C. A. Mead, "A physical charge-controlled model for MOS transistors", in P. Losleben, (ed), *Advanced Research in VLSI*. Cambridge, MA: MIT Press, 1987.

[5] Y. P. Tsvividis and K. Suyama, "MOSFET modeling for analog circuit CAD: problems and prospects", *IEEE J. Solid State Circuits*, vol.29, pp. 210-216, 1994.

[6] C. C. Enz, F. Krummenacher, and E. A. Vittoz, "An analytical MOS transistor model valid in all regions of operation and dedicated to low-voltage and low-current applications", *Analog Integrated Circuits and Signal Processing*, vol.8, pp. 83-114, 1995.

[7] Y. Tsvividis, "Operation and modeling of the MOS transistor". New York: McGraw-Hill, 1987.